Chemical Physics 377 (2010) 1–5

Contents lists available at ScienceDirect

Chemical Physics

journal homepage: www.elsevier.com/locate/chemphys

High resolution X-ray emission spectroscopy of water and aqueous ions using the micro-jet technique

Kathrin M. Lange [a], René Könnecke [a,1], Samira Ghadimi [a], Ronny Golnak [a], Mikhail A. Soldatov [a,b], Kai F. Hodeck [a], Alexander Soldatov [b], Emad F. Aziz [a,c,*]

[a] Helmholtz-Zentrum Berlin für Materialien und Energie, c/o BESSY GmbH, Albert-Einstein-Strasse 15, 12489 Berlin, Germany
[b] Research Center for Nanoscale Structure of Matter, Southern Federal University, Sorge 5, Rostov-na-Donu 344090, Russia
[c] Freie Universität Berlin, FB Physik, Arnimallee 14, D-14195 Berlin, Germany

ARTICLE INFO

Article history:
Received 23 August 2010
In final form 30 August 2010
Available online 20 September 2010

Keywords:
XES
Soft X-ray
Micro-jet
Water
Ions

ABSTRACT

Soft X-ray absorption (XA) and emission (XE) spectroscopy is a powerful method for probing the local electronic structure of light elements (e.g. C, O, N, S) and transition metals, which are all of importance for biochemical systems. Here, we report for the first time on the XE spectra of a liquid micro-jet sample in a vacuum environment. We developed a high resolution X-ray emission spectrometer and recorded the spectra of pure water in full agreement with those of the literature, as well as of an aqueous solution of $NiCl_2$. For the latter system, ground state Hartree–Fock calculations using a self-consistent reaction field (SCRF) approach were carried out to specify the nature of the d-occupied orbital. Our results confirm the dark-channel-fluorescence-yield mechanism that we recently proposed for the case of metal ions in aqueous solutions. The ability to record absorption and emission spectra of an aqueous liquid-jet opens the way for the study of biochemical systems in physiological media.

1. Introduction

Spectroscopic techniques based on photon-in/photon-out processes using synchrotron radiation have proven to be highly sensitive tools for investigating the local electronic structure of condensed matter and of chemical and biological systems. Soft X-ray absorption [1–9] and emission spectroscopy [10–14] of liquid systems can probe the elements of life as e.g. C, O and N through the K-edges [1,8,11,15] and transition metals through the L-edges [5,16,17]. Recently, the XAS technique was further extended for investigating in situ the preparation process of solar cells [18,19], as well as for probing the transition metal active centre of proteins and enzymes under physiological conditions [16,17,20]. In most of these recent XA studies on liquids, the samples were contained in a cell consisting of soft X-ray transparent thin (few hundreds of nm's) membrane windows made of silicon nitride (Si_3N_4). Flowing the liquid behind the membrane, as can be done with flow-cells, additionally reduces the risks of sample damage with respect to static drop-behind-membrane cells. However, in using a membrane several issues have to be considered: (i) the membrane should be ideally transparent for the respective fluorescence light of interest. Therefore elements that are contained in the membrane material (Si and N) or are energetically close to them are not directly measurable. (ii) Since no membrane is ideally transparent for any energy range, measuring techniques which require a high incoming flux like, e.g. X-ray emission spectroscopy (XES), suffer from the loss of photons leading to long data acquisition times [3]. In the case of very low concentration samples, such as biochemical systems in physiological media, the loss of intensity is detrimental [16,17,20]. (iii) Interactions with the membrane, like hydrophobic or hydrophilic effects can induce artifacts in the spectra. As mentioned in the literature, the membrane can also react chemically upon X-ray radiation with the sample (e.g. oxidization of the inner surface of the Si_3N_4 membrane) and change its nature as a function of irradiation [14]. Such changes may affect the XA and XE spectra and cannot be neglected.

To overcome these issues, in this work fluorescence yield XAS and XES are combined for the first time with the micro-jet technique. We demonstrate this new approach by investigating the oxygen K-edge of liquid water and the Ni L-edge of an $NiCl_2$ aqueous solution under resonant and non-resonant excitation. We present our preliminary results to demonstrate the capability of our new setup. A detailed discussion of our results, in particular for the case of aqueous Ni^{2+} ions will be given later. The series of XE spectra of water measured from the liquid-jet give qualitatively the same characteristics as what has been shown before for water

* Corresponding author at: Helmholtz-Zentrum Berlin für Materialien und Energie, c/o BESSY GmbH, Albert-Einstein-Strasse 15, 12489 Berlin, Germany. Fax: +49 3063924757.
E-mail address: Emad.Aziz@helmholtz-berlin.de (E.F. Aziz).
[1] K.M.L. and R.K. contribute equally to this work.

0301-0104/$ - see front matter © 2010 Elsevier B.V. All rights reserved.
doi:10.1016/j.chemphys.2010.08.023

behind an Si_3N_4 membrane and show a resolution comparable to the most recent publications on high resolution XES [10,14]. For the aqueous $NiCl_2$, concentrations down to 250 mM were measured, but according to the signal to noise ratio, even lower ion-concentrations can be measured with this setup. Moreover, the emission lines reflect what we recently proposed as the dark-channel-fluorescence-yield (DCFY) mechanism [21], which reveals electron delocalization in mixed orbitals between water and nickel. For the interpretation of the emission spectra of aqueous $NiCl_2$, theoretical calculations using a Hartree–Fock (HF) approach combined with a self-consistent reaction field (SCRF) to include solvent effects were carried out.

2. Experimental setup (LiXEdrom)

The samples were measured with the LiXEdrom-setup at the U41 PGM beamline of BESSY. This spectrometer was developed for investigating liquid samples using the micro-jet technique. The XA spectra were recorded in the total fluorescence yield (TFY) mode with a GaAs diode (grounded and with shielded connections to avoid disturbing signals from electrons). For the XE measurements a Gamma Data MCP-CCD-detector combined with a self-developed grating holder was used in Rowland-geometry in a slit-less configuration (see Fig. 1a). By rotation of the holder, it can be chosen between four different blazed gratings covering the energy range from 20 to 1000 eV (G1: energy range: 20–50 eV, line density: 400 lines mm^{-1}, radius: 2 m; G2: energy range: 50–175 eV, line density: 600 lines mm^{-1}, radius: 3.71 m; G3: energy range: 175–400 eV, line density: 1200 lines mm^{-1}, radius: 5 m and G4: energy range: 400–1000 eV, line density: 1200 lines mm^{-1}, radius: 7.5 m). The spectra shown in this work were recorded with the G4 grating. The resolution reached with this configuration is comparable to recently published high resolution XES measurements of 350 meV at 530 eV [10,14]. For the measurements of liquid water and $NiCl_2$ in aqueous solution a 23 μm and an 18 μm nozzle were used for the liquid-jet, respectively. The pressure inside the liquid-jet chamber during the measurements was in the range of 10^{-5}–10^{-6} mbar. Note, that the use of the liquid-jet technique allows measuring always a fresh sample, so that X-ray induced heating or sample damage is avoided. The electron yield (EY) spectra of aqueous $NiCl_2$ obtained from the liquid-jet were recorded as described before [22].

3. Theoretical calculation

To reveal the nature of the molecular orbitals (MOs) of Ni^{2+} in water which are involved in the XE spectra we carried out ground state Hartree–Fock (HF) calculations using the Gaussian03 program package [23]. An often followed approach to include solvent effects into high level *ab initio* calculations are self-consistent reaction field (SCRF) methods. In these methods, the solvent is modeled as a continuum of uniform dielectric constant (called the reaction field) and the solute is placed into a cavity within the solvent. The different SCRF models differ in how they define the cavity and the reaction field. In this study we used the Onsager reaction field model where Ni^{2+} occupies a fixed spherical cavity of radius a_0 within the solvent field. A dipole of the molecule will induce a dipole in the medium. On the other hand, the electric field applied by the solvent will interact with the molecular dipole causing stabilization for the system.

4. Results and discussion

In the following the results of the measurements obtained from liquid water will be discussed and compared to the recently published high resolution spectra of water [10,14]. In the second section, we will present the XE spectra obtained from Ni^{2+} resonant excitation around the L_3-edge of $NiCl_2$ aqueous solution. We will compare these results with our results from drop-behind-membrane measurements at beamline 7, ALS-Berkeley lab [3] and verify the validity of the DCFY mechanism that we recently proposed [21].

4.1. Pure water

Using the example of liquid water we show in this section, that our newly developed liquid-jet XES spectrometer achieves a resolution comparable to the most recent published high resolution XES measurements carried out on membrane cells [10,14]. In the top of Fig. 2 the XA spectrum of H_2O obtained with the micro-jet

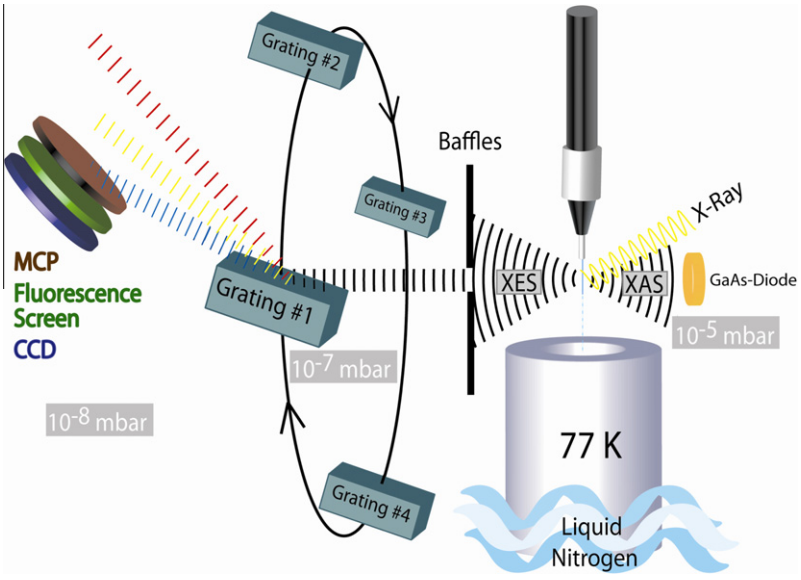

Fig. 1. Schematic drawing of (a) the LiXEdrom-setup with liquid sample delivered via a micro-jet and trapped inside a container cooled down by liquid nitrogen. The emitted light is collected via total fluorescence yield (TFY–XAS) or energy dispersed (XE) with the help of blazed gratings.

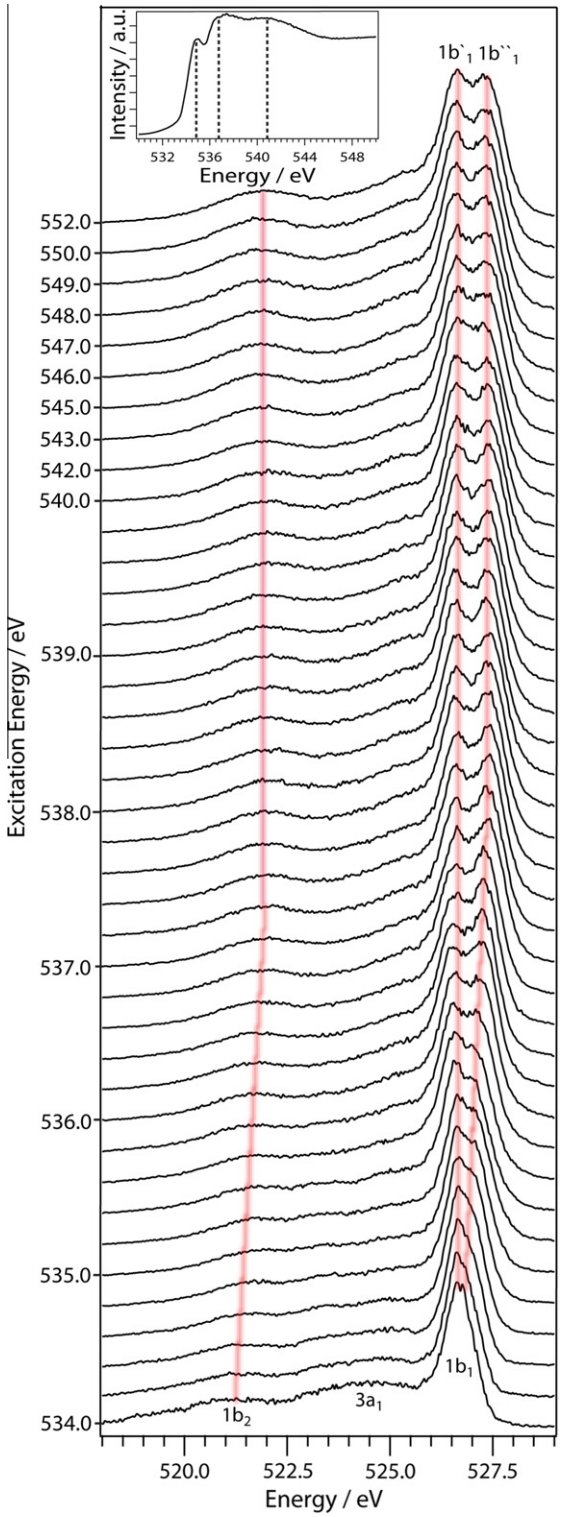

Fig. 2. O1s X-ray emission spectra of pure liquid water (15 °C) collected from the micro-jet at excitation energies from 534 eV up to 552 eV with 0.2 eV energy steps presented on the *Y*-axis; Inset: X-ray absorption spectrum of pure liquid water (15 °C) collected from the micro-jet with the main excitation energies marked.

is presented, showing three characteristic spectral features: the pre-edge, the main-edge and the post-edge around 535, 537.5 and 540 eV, respectively. Note, that because of self-absorption effects the pre- and post-edge features are overemphasized with respect to the main-edge feature. The XES mapping, beginning with the resonant excitation of the pre-edge at 534 eV and proceeding upwards in 0.2 eV steps, is shown in the bottom part of Fig. 2. Whereas XAS probes the unoccupied density of electronic states, XES reveals information about the occupied electronic states, which for water are the $1b_2$, $3a_1$ and the $1b_1$ molecular orbitals (MO). The apparent broadening of the spectral features of the binding $1b_2$, $3a_1$ orbitals in comparison to non-bonding lone-pair $1b_1$ orbital is due to core–hole-induced proton transfer dynamics. Upon increasing the excitation energy a splitting of the $1b_1$ spectral feature into the two peaks $1b_1'$ and $1b_1''$ sets in. Whereas the former remains at its energetic position, the latter blue-shifts upon raising the excitation energy to 537 eV. For higher excitation energies the splitting of the two peaks stays constant. The origin of this splitting is much discussed in the literature. One interpretation correlates the two features to different hydrogen bonding states of the water molecule [10]. Another explanation proposes that ultrafast dissociation is causing the splitting, so that the $1b_1'$ can be correlated to dissociated OH species and the $1b_1''$ to intact water molecules [14].

Regarding the agreement of our experimental data obtained from the liquid-jet to the measurements of membrane cells, we can conclude, that the latter results are not affected by long-range effects caused by the hydrophobic or hydrophilic interactions with the membrane. In the same way we can conclude, that our measurements on the liquid-jet are not suffering from a thermodynamic disequilibrium as was suspected by Weinhardt et al. [14].

4.2. Aqueous solution of Ni^{2+}

Recently we reported on a new mechanism for the electron transfer in aqueous metal-based atomic and molecular ions, focusing on the case of iron [21]. XA spectra obtained from aqueous transition metal L-edges by total fluorescence yield (TFY) measurements showed distortions compared to the respective non-aqueous transition metal solution spectra. Some of the TFY spectral components to turned below the background of fluorescence light from the solvent, appearing as dips. The dips were attributed to an electron transfer from the X-ray excited state of the solute to the water molecules. The electron transfer occurs from states that delocalize in the electronic structure of the water continuum. We called the delocalized channel a "dark channel" and the respective mechanism the "dark-channel-fluorescence-yield" (DCFY). This observation was stressing the role of the water molecule, with respect to the other solvents, as it affects the electronic structure of the solute by forming a complex with its molecular orbitals. It was however stressed that any efficient electron transfer is correlated to a reduction of the fluorescence and that the DCFY is not necessarily depending on the water solvent. Examples where dips appear in the TFY spectra include metal-based molecular complexes undergoing intramolecular electron transfer [21].

The excited intermolecular electron transfer from the metal to the water molecule reduces the X-ray fluorescence yield from the metal. However, the decay is largely (more than 99%) dominated by Auger processes. Therefore, the comparison of FY and electron yield (EY) spectra of aqueous transition metals should also show directly the distortion caused by the DCFY. In this study we show that L-edge XA spectrum of the aqueous solution of Ni^{2+} obtained from FY-technique differs from the one based on the EY-technique at the L_3-edge at 851.5 eV (see Fig 3a). In general, the 2p (L-edge) spectrum of Ni^{2+} splits into two main regions, the L_3-edge around 852 eV and the L_2-edge around 869 eV. Whereas the peaks at 851.5 eV as well as 868.5 eV are related to a $2p^53d^9$ final state of triplet character, the peaks at 853.8 and 869.8 eV are related to a singlet final state [5]. Accordingly, the splitting between the triplet and the singlet states is 2.3 eV, as shown schematically in Fig. 3c Interestingly, only the triplet state at 851.5 eV is showing a loss of intensity in the FY-spectrum in comparison to the EY-spectrum, which we attribute to a weak DCFY, because in a strong DCFY as for

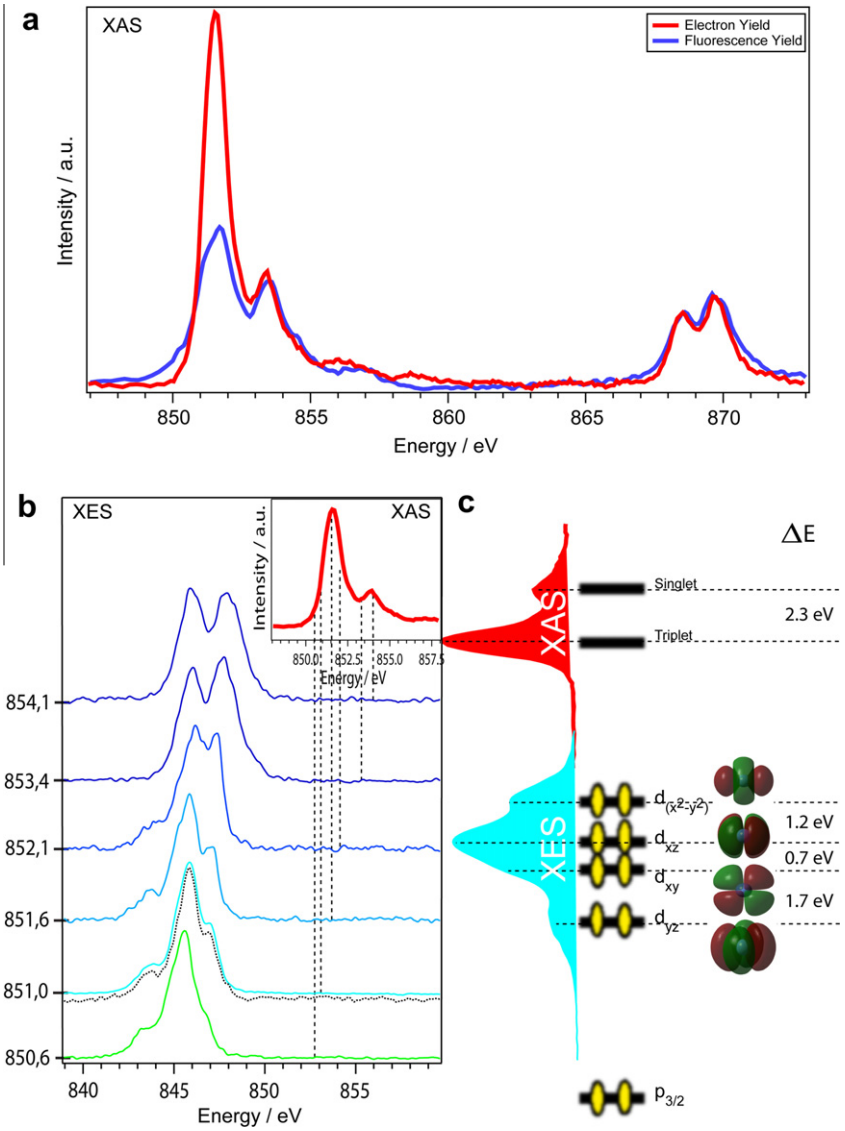

Fig. 3. Ni-2p X-ray absorption and emission spectra of 1 M aqueous $NiCl_2$; (a) comparison between total fluorescence yield and total electron yield XA spectra, (b) emission spectra at different excitation energies labeled in the inset XA spectrum of Ni-2p. For the excitation energy of 851, 0 eV also the spectrum of a 0.25 M aqueous $NiCl_2$ sample is shown (dashed line), and (c) schematic picture of the occupied and unoccupied Ni-orbitals of in aqueous $NiCl_2$ as obtained experimentally from the XA and XES measurements. The assignment of the orbitals is based on ground state HF-SCRF calculations.

the iron ions the spectral features turn to dips [21], as already mentioned. This distortion is not reproduced by the triplet state at the L_2-edge, due to a shorter core–hole lifetime (L_2-edge < 1 fs, L_3-edge ~ 3 fs) [24] reducing with its higher radiative decay rate the probability of an electron transfer. This sets an upper limit of ~2 to 2.5 fs for the electron transfer time to the solvent, since mainly the low-energy peak of the L_3-edge showed distortions. Using XES it is possible to observe the occupied MOs that correspond to the relaxation channels upon excitation into the mixed orbitals. The XE spectra obtained of the 1 M aqueous $NiCl_2$ upon increasing the excitation energy stepwise from 850.6 eV up to 854.1 eV are shown in Fig. 3b. In order to investigate the concentration dependence and the achievable signal to noise ratio for the jet-measurements, also 250 mM $NiCl_2$ in water were measured. Since the XES lines did not change much with respect to the high concentration case, we show in Fig. 3b one spectrum at excitation energy of 851 eV. In Fig. 3c, the occupied d-orbitals as obtained for 851 eV excitation energy are presented schematically. The dashed lines correspond to the experimental peak positions. Using ground state HF calculations combined with the SCRF approach, the experimental peaks are correlated to the respective d-orbitals and were labeled accordingly in Fig. 3c. Despite the ground state calculation, the theoretical calculations are in good agreement with the experimental results; however the theory shows d_{xy} and d_{xz} at the same energy ($\Delta E = 0$). Briefly, ΔE obtained by HF between d_{yz} and d_{xy} or d_{xz} is 2.5 eV, whereas the experimental ΔE from d_{yz} to d_{xz} is 2.4 eV. Furthermore, ΔE obtained by HF from d_{xy} or d_{xz} to $d_{(x^2-y^2)}$ is 1.0 eV, whereas the corresponding experimental value is 1.2 eV.

In Fig. 3b the emission spectra upon excitation into the triplet state (which is affected by DCFY) are shown for excitation energies from 850.6 eV up to 852.1 eV. In the respective spectra the emission lines of all the above mentioned d-MOs are observed (see assignments in Fig. 3c). Upon exciting resonantly the electron to the singlet state, we obtained XE spectra with only two peaks (see Fig. 3b, excitation energies 853.4–854.1 eV). The peak correlated to the d_{yz} MO disappeared. According to the DCFY effects shown in the EY–FY comparison for this system, there are mixed Ni–water orbitals formed upon solvation. Upon excitation, the electron can delocalize in these mixed orbitals. If the lifetime of the respective excited state is sufficient, as it is for the triplet state,

emission from all occupied d-orbitals is observed. On the other hand, for the singlet excited state with its shorter lifetime no relaxation from the d_{yz} takes place.

Interestingly, upon going to higher excitation energies a blue-shift of the peak correlated to the $d_{(x^2-y^2)}$ MO is observed going along with an increase of intensity. The $d_{(x^2-y^2)}$ MO is the highest of the occupied d-orbitals and therefore most involved in the interaction with the solvent. In principle, one can describe the bond between the Ni^{2+} and the water as semi-covalent bond, according to the MOs mixing pictures drawn here. The intensity increase and the energy shifting of the corresponding spectral feature could be therefore explained by vibronic coupling effects, affecting most the bonding orbitals [2]. Also a blue-shifting of the d_{xy}, d_{xz} and d_{yz} spectral features is observed upon increasing the excitation energy from 850.6 to 852.1. Upon excitation to the singlet state, this systematic shifting is not observed. For a clearer understanding of these effects, however, more systematic studies are required including variation of the solvent.

From the presented measurements the advantage of the micro-jet technique becomes obvious. Comparing the measuring time for the $NiCl_2$ spectra obtained from samples in a cell equipped with Si_3N_4 membrane [3] to the present ones, it was possible to reduce the data acquisition time down to a quarter. A time-dependent chemical reaction with the sample cannot be excluded for the membrane measurements. For larger organic or biological molecules this effect can be significant. Actually, the technique of using the thin membrane can be quite successful under two circumstances, first, short measuring times (in the range of minutes) and second, extensive cleaning between samples with the solvent of choice. Usually these requirements cannot be fulfilled using the XES technique, as for diluted samples (typical for biological and chemical applications) XE spectra can take up to many hours.

5. Conclusion

Our new high resolution XE and XA spectrometer (LiXEdrom) setup for probing the local electronic structure of elements in aqueous solution has been used with a soft X-ray synchrotron light source and the micro-jet technique. With the advantages of the beamline U41-PGM at BESSY II, a small focus and a high flux, the spectrometer is able to probe freshly introduced liquid samples avoiding X-ray induced sample damage. As a demonstration of its capability, in this study we presented two examples of XES results for the application of this spectrometer; (A) liquid water, where we show that our spectra from the micro-jet agree well with the high resolution XES measurements presented recently in the literature. From this, we can conclude that for water there are no long-range effects induced by the membrane affecting the spectra as well as no thermodynamic disequilibrium induced by the jet. (B) For an aqueous solution of $NiCl_2$, we show that due to a membrane-less configuration a significant reduction of measuring time is achieved. Moreover, we show in this work directly the spectral distortion of XA–FY spectra caused by the recently proposed DCFY mechanism by comparison to EY spectra of aqueous $NiCl_2$ samples obtained from the liquid-jet. The vibronic-coupling in the XES peaks give an evidence for the semi-covalent bond between the Ni^{2+} and the water hydration.

Acknowledgments

The authors thank to Prof. Dr. Jan-Eric Rubbensson for his advices during the building of the XE spectrometer, Dr. Carlo Callegari, Agne Sulciute and Rafael Vescovi for their help during the beamtime and the entire workshop at BESSY/HZB for their support. We acknowledge support of the German-Russian Interdisciplinary Science Center (G-RISC) and the Helmholtz-Gemeinschaft through the young investigator fund VH-NG-635.

References

[1] P. Wernet, D. Nordlund, U. Bergmann, M. Cavalleri, M. Odelius, H. Ogasawara, L.A. Näslund, T.K. Hirsch, L. Ojamae, P. Glatzel, L.G.M. Pettersson, A. Nilsson, Science 304 (2004) 995.
[2] J. Grasjo, E. Andersson, J. Forsberg, E.F. Aziz, B. Brena, C. Johansson, J. Nordgren, L. Duda, J. Andersson, F. Hennies, J.E. Rubensson, P. Hansson, J. Phys. Chem. B 113 (2009) 8201.
[3] E.F. Aziz, J. Electron Spectrosc. Relat. Phenom. 177 (2010) 168.
[4] E.F. Aziz, W. Eberhardt, S. Eisebitt, Z. Phys. Chem. 222 (2008) 727.
[5] E.F. Aziz, S. Eisebitt, F. de Groot, J. Chiou, C. Dong, J. Guo, W. Eberhardt, J. Phys. Chem. B 111 (2007) 4440.
[6] E.F. Aziz, S. Eisebitt, W. Eberhardt, L. Cwiklik, P. Jungwirth, J. Phys. Chem. B 112 (2008) 1262.
[7] E.F. Aziz, M. Freiwald, S. Eisebitt, W. Eberhardt, Phys. Rev. B 73 (2006) 75120.
[8] E.F. Aziz, N. Ottosson, S. Eisebitt, W. Eberhardt, B. Jagoda-Cwiklik, R. Vacha, P. Jungwirth, B. Winter, J. Phys. Chem. B 112 (2008) 12567.
[9] E.F. Aziz, A. Zimina, M. Freiwald, S. Eisebitt, W. Eberhardt, J. Chem. Phys. 124 (2006) 114502.
[10] T. Tokushima, Y. Harada, Y. Horikawa, O. Takahashi, Y. Senba, H. Ohashi, L.G.M. Pettersson, A. Nilsson, S. Shin, J. Electron Spectrosc. Relat. Phenom. 177 (2010) 192.
[11] J.H. Guo, Y. Luo, A. Augustsson, S. Kashtanov, J.E. Rubensson, D.K. Shuh, H. Agren, J. Nordgren, Phys. Rev. Lett. 91 (2003) 157401.
[12] J.H. Guo, A. Augustsson, S. Kashtanov, D. Spangberg, J. Nordgren, K. Hermansson, Y. Luo, A. Augustsson, J. Electron Spectrosc. Relat. Phenom. 144–147 (2005) 287.
[13] J.H. Guo, Y. Luo, A. Augustsson, J.E. Rubensson, C. Sathe, H. Agren, H. Siegbahn, J. Nordgren, Phys. Rev. Lett. 89 (2002) 137402.
[14] L. Weinhardt, O. Fuchs, M. Blum, M. Bar, M. Weigand, J.D. Denlinger, Y. Zubavichus, M. Zharnikov, M. Grunze, C. Heske, E. Umbach, J. Electron Spectrosc. Relat. Phenom. 177 (2010) 206.
[15] E.E. Aziz, A. Vollmer, S. Eisebitt, W. Eberhardt, P. Pingel, D. Neher, N. Koch, Adv. Mater. 19 (2007) 3257.
[16] D. Panzer, C. Beck, M. Hahn, J. Maul, G. Schonhense, H. Decker, E.F. Aziz, J. Phys. Chem. Lett. 1 (2010) 1642.
[17] E.F. Aziz, N. Ottosson, S. Bonhommeau, N. Bergmann, W. Eberhardt, M. Chergui, Phys. Rev. Lett. 102 (2009) 68103.
[18] I. Lauermann, T. Kropp, D. Vottier, A. Ennaoui, W. Eberhardt, E.F. Aziz, ChemPhysChem 10 (2009) 532.
[19] S.M. Greil, I. Lauermann, A. Ennaoui, T. Kropp, K.M. Lange, M. Weber, E.F. Aziz, Nucl. Instrum. Methods Phys. Res. Sect. B 268 (2010) 263.
[20] N. Bergmann, S. Bonhommeau, K.M. Lange, S.M. Greil, S. Eisebitt, F. de Groot, M. Chergui, E.F. Aziz, Phys. Chem. Chem. Phys. 12 (2010) 4827.
[21] E.F. Aziz, S. Bonhommeau, M. Chergui, Nature Chemistry (2010), doi:10.1038/nchem.768.
[22] K.R. Wilson, B.S. Rude, J. Smith, C. Cappa, D.T. Co, R.D. Schaller, M. Larsson, T. Catalano, R.J. Saykally, Rev. Sci. Instrum. 75 (2004) 725.
[23] M.J. Frisch, G.W. Trucks, H.B. Schlegel, G.E. Scuseria, M.A. Robb, J.R. Cheeseman, V.G. Zakrzewski, J.A. Montgomery, R.E. Stratmann, J.C. Burant, S. Dapprich, J.M. Millam, A.D. Daniels, K.N. Kudin, M.C. Strain, O. Farkas, J. Tomasi, V. Barone, M. Cossi, R. Cammi, B. Mennucci, C. Pomelli, C. Adamo, S. Clifford, J. Ochterski, G.A. Petersson, P.Y. Ayala, Q. Cui, K. Morokuma, P. Salvador, J.J. Dannenberg, D.K. Malick, A.D. Rabuck, K. Raghavachari, J.B. Foresman, J. Cioslowski, J.V. Ortiz, A.G. Baboul, B.B. Stefanov, G. Liu, A. Liashenko, P. Piskorz, I. Komaromi, R. Gomperts, R.L. Martin, D.J. Fox, T. Keith, M.A. Al-Laham, C.Y. Peng, A. Nanayakkara, M. Challacombe, P.M.W. Gill, B. Johnson, W. Chen, M.W. Wong, J.L. Andres, C. Gonzalez, M. Head-Gordon, E.S. Replogle, J.A. Pople, Gaussian 03, Windows 03 ed., Pittsburgh, PA, 2003.
[24] M. Ohno, G.A. van Riessen, J. Electron Spectrosc. Relat. Phenom. 128 (2003) 1.